

Optical doping of soda-lime-silicate glass with erbium by ion implantation

E. Snoeks, G. N. van den Hoven, and A. Polman

FOM Institute for Atomic and Molecular Physics, Kruislaan 407, 1098 SJ Amsterdam, The Netherlands

(Received 6 January 1993; accepted for publication 2 March 1993)

Soda-lime-silicate glass has been implanted with 500 keV Er ions at fluences between 8.6×10^{14} and $1.8 \times 10^{16}/\text{cm}^2$ with the aim to optically dope the material in the near surface region. The ion range was 100 nm, and Er concentrations in the range 0.09–1.9 at. % were obtained. The characteristic photoluminescence (PL) of Er^{3+} around $1.54 \mu\text{m}$ is observed at room temperature in as-implanted glass. The PL intensity increases by an order of magnitude after annealing above 500°C , as a result of annihilation of implantation-induced defects. Annealing causes an increase in PL lifetime. As a function of Er fluence, the PL intensity first increases, but levels off above $\sim 6 \times 10^{15} \text{Er}/\text{cm}^2$ (0.6 at. % Er peak concentration). The PL lifetime decreases from 13 to 1.5 ms for increasing Er concentration. The decrease in PL efficiency with concentration is attributed to concentration quenching caused by Er-Er interactions. The optimal combination of PL intensity and lifetime is reached at ≈ 0.4 at. % peak concentration, for which the lifetime is 6 ms. For high Er concentrations and high pump intensities ($\sim 3 \text{kW}/\text{cm}^2$) an additional, intensity dependent quenching mechanism (possibly cooperative upconversion) is observed.

I. INTRODUCTION

Erbium-doped materials have recently become of great interest because of their use as optical gain media.¹ Erbium shows an optical transition (intra- $4f$) around $1.5 \mu\text{m}$ (Fig. 1), a standard wavelength in silica-based optical fiber communication systems. Optical fibers have been doped with Er to fabricate lasers, and in 1987 the first Er-doped fiber amplifiers operating around $1.5 \mu\text{m}$ were reported.² While fiber compatibility is important for long-distance communication systems, on a local scale where optical switching and multiplexing are performed using planar waveguide structures,³ it would be desirable to integrate a planar Er-based amplifier. For example, a planar amplifier with a moderate gain could compensate for the intensity decrease in a one-to-two beam splitter.

Various methods have been used to fabricate Er-doped planar silica waveguides, and in some cases optical gain has been demonstrated.⁴⁻⁶ In this article we use ion implantation to dope soda-lime-silicate glass with Er. An important advantage of this glass over other materials is that low-loss fiber-compatible planar waveguides can be fabricated by the relatively simple $\text{Na}^+ \leftrightarrow \text{K}^+$ ion-exchange process.^{7,8} A further advantage of using a multicomponent glass is that it may accommodate larger concentrations of Er^{1,9} than, for example, pure silica in which precipitation effects have been observed at concentrations of 0.1 at. %.¹⁰

In this work we investigate 500 keV Er-implanted soda-lime-silicate glass. The dependence of photoluminescence spectra, intensity, and lifetime on Er concentration and post-implantation anneal temperature are studied. Annealing above 500°C is required to annihilate the implantation-induced defects. For high Er concentration the luminescence is quenched, possibly due to Er-Er interactions. The optimum combination of luminescence lifetime and intensity is obtained at an Er peak concentration of ≈ 0.4 at. %.

II. EXPERIMENT

Commercially available soda-lime-silicate glass (Fisher Premium), 1 mm thick, was implanted at room temperature with 500 keV Er ions. The ion current density on sample was $\sim 0.5 \mu\text{A}/\text{cm}^2$, and the implanted fluences ranged from 8.6×10^{14} to $1.8 \times 10^{16}/\text{cm}^2$. To avoid electrical charging of the glass during ion irradiation, a 420 \AA Al film was evaporated on the glass surface. It was etched off in a NaOH solution after implantation. Thermal annealing was performed in a tube furnace at a base pressure below 5×10^{-7} mbar, at temperatures ranging from 300 to 650°C . All anneals were done for one hour.

Erbium concentration profiles were determined by Rutherford backscattering spectrometry (RBS) using $2.0 \text{ MeV } ^4\text{He}^+$ and a scattering angle of 169° . Photoluminescence (PL) spectroscopy was carried out at room temperature, with the 514.5 nm line of an Ar-ion laser as excitation source. This line is absorbed in the $^2H_{11/2}$ manifold of Er^{3+} (see Fig. 1). Powers between 70 and 350 mW were used in a $\sim 0.3 \text{ mm}$ diameter spot, for which no beam heating of the samples was observed. The luminescence signal was spectrally analyzed with a 48 cm monochromator, and detected with a liquid-nitrogen-cooled Ge detector, yielding a spectral resolution of 2.3 nm. The pump beam was chopped at 12 Hz and spectra were recorded using a lock-in amplifier. Time-resolved luminescence decay measurements were performed using a 1.5 ms, 1.4 W pump pulse with a cutoff time shorter than $150 \mu\text{s}$. Decay data were recorded and averaged using a digitizing oscilloscope system.

III. RESULTS

Figure 2 shows an RBS spectrum of soda-lime-silicate glass after implantation of $5.4 \times 10^{15} \text{Er}/\text{cm}^2$. The sharp peak at channel 269 corresponds to the Al coating. This coating causes a shift over five channels of the edges in the

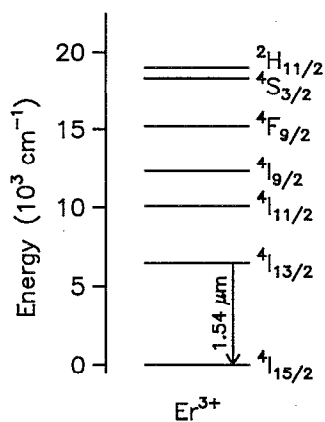


FIG. 1. Energy-level diagram of Er^{3+} free ion (see Ref. 12). When Er^{3+} is incorporated in a solid, the levels are splitted into manifolds due to the Stark effect.

spectrum with respect to the indicated surface channels. The composition of the multicomponent glass as determined from this spectrum, agrees with the specified composition (in mol %: 72.2 SiO_2 , 14.3 Na_2O , 6.4 CaO , 1.2 K_2O , and small quantities of Al_2O_3 , MgO , and others). Earlier experiments¹¹ have shown that ion implantation of alkali silicate glass can cause a depletion of alkali atoms in the surface region. However, no Na loss is observed in our experiments, which may be a consequence of the presence of the Al coating. The Er profile is nearly Gaussian shaped, and peaks at about 100 nm depth from the glass surface, with a full width at half-maximum (FWHM) of 90 nm, assuming a soda-lime-silicate glass density of 7.8×10^{22} atoms/cm³. The peak concentration is 0.6 at. %. Samples implanted at other fluences show similarly shaped profiles, with peak concentrations ranging from 0.09 to 1.9 at. %.

Figure 3 shows a PL spectrum of Er-implanted (3.7×10^{15} /cm²) soda-lime-silicate glass, after annealing

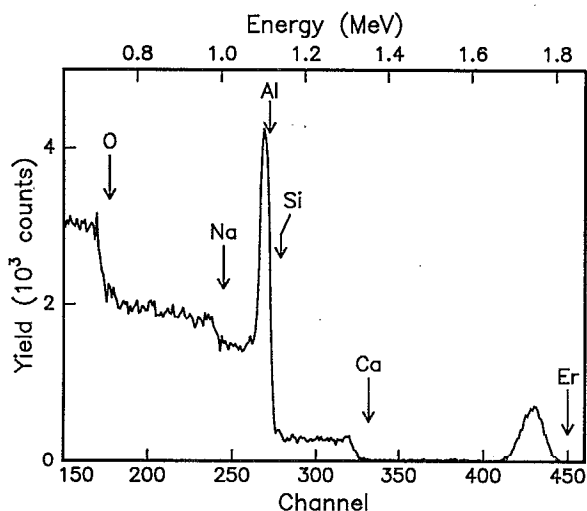


FIG. 2. RBS spectrum of Er-implanted (5.4×10^{15} Er/cm²) soda-lime-silicate glass with a 420 Å Al coating. The arrows indicate surface channels of the various glass constituents.

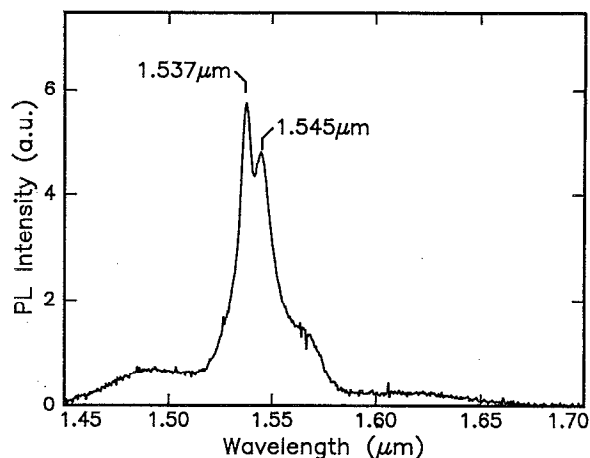


FIG. 3. Room-temperature photoluminescence spectrum of Er-implanted (3.7×10^{15} /cm², 0.4 at. % peak concentration) soda-lime-silicate glass after thermal annealing at 512 °C. Pump power=70 mW, $\lambda_{\text{pump}}=514.5$ nm, spectral resolution=2.3 nm.

at 512 °C for 1 h. The spectrum shows peaks at the wavelengths (λ) of 1.537 and 1.545 μm and broad shoulders extending from roughly 1.45 to 1.67 μm . This emission is characteristic for the intra- $4f$ transitions between the $^4I_{13/2}$ and $^4I_{15/2}$ manifolds of Er^{3+} (see Fig. 1).¹² The width of the spectrum is 19 nm FWHM. Spectra were also measured for samples implanted at other fluences and annealed at different temperatures. The shape of these spectra does not significantly deviate from the spectrum shown in Fig. 3.

The PL intensity depends strongly on the temperature of the annealing treatment after implantation. Figure 4 shows peak intensities, measured at $\lambda = 1.537 \mu\text{m}$, for samples annealed at temperatures in the range 300–600 °C.

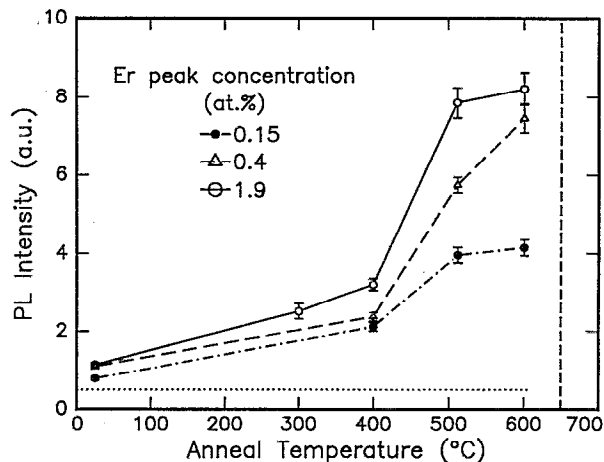


FIG. 4. Room-temperature photoluminescence peak intensity at $\lambda = 1.537 \mu\text{m}$ as a function of anneal temperature for samples implanted with 1.3, 3.7, and 18×10^{15} Er/cm² (0.15, 0.4, and 1.9 at. % peak concentration). The lines serve as guides for the eye. The dotted line shows the background luminescence of unimplanted samples. The dashed vertical line at 650 °C marks the point at which the glass surface starts to deform.

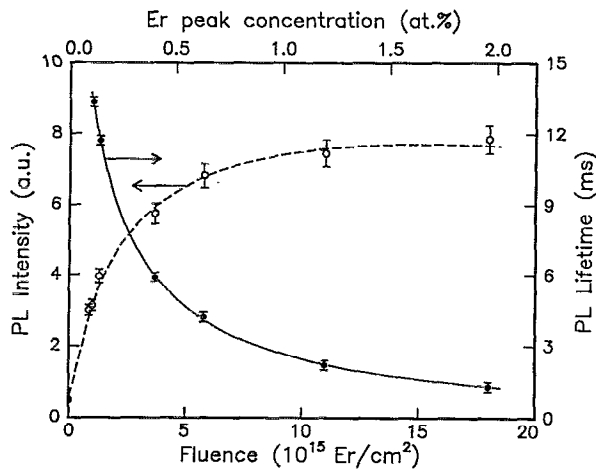


FIG. 5. Photoluminescence peak intensity (open data points, left axis) and lifetime (solid data points, right axis) at $\lambda = 1.537 \mu\text{m}$ as a function of Er fluence. All samples were annealed at 512°C in vacuum. The Er peak concentrations are indicated on the top axis. The solid line is a guide for the eye, the dashed line is calculated from the solid line using Eq. (1).

Data are shown for samples with Er peak concentrations of 0.15, 0.4, and 1.9 at. %. As can be seen, unannealed samples show a relatively low PL intensity. Thermal annealing at temperatures up to 512°C increases the PL intensity. A smaller further increase is observed for 600°C annealing. It should be noted that the unimplanted glass also shows a very low PL signal, as a result of trace levels of Er in the bulk (<0.1 ppm). This background signal was the same for all samples, and is indicated in Fig. 4 by the dotted line. The dashed vertical line at 650°C indicates the temperature at which macroscopic deformation of the glass was observed. The softening point specified for this glass is 692°C .

It is clear from Fig. 4 that the maximum PL intensity after 512°C annealing does not scale linearly with the Er fluence. Increasing the Er peak concentration from 0.15 to 1.9 at. % only doubles the PL intensity. Figure 5 shows the PL intensity of implanted samples annealed at 512°C as a function of Er fluence (open datapoints). The PL intensity increases almost linearly with fluence for fluences smaller than $2 \times 10^{15}/\text{cm}^2$. At higher Er fluences the intensity increase levels off, and a saturation is observed above $\sim 6 \times 10^{15}/\text{cm}^2$, corresponding to an Er peak concentration of 0.6 at. %.

Figure 6 shows PL decay measurements for samples with Er peak concentrations of 0.15, 0.4, and 1.9 at. %, annealed at 512°C . As can be seen, the PL decay depends strongly on the Er concentration. First, the lifetime decreases with increasing concentration. The e^{-1} decay-times for the curves in Fig. 6, together with data for other Er fluences, are plotted as solid data points against the right-hand scale in Fig. 5. Second, the shape of the decay curves changes. For low concentrations, the decay is nearly single exponential, but as the Er concentration increases, the curves deviate from single exponential behavior. This is partly a result of the fact that the Er concentration profiles are Gaussian shaped: the PL decay curve is composed of

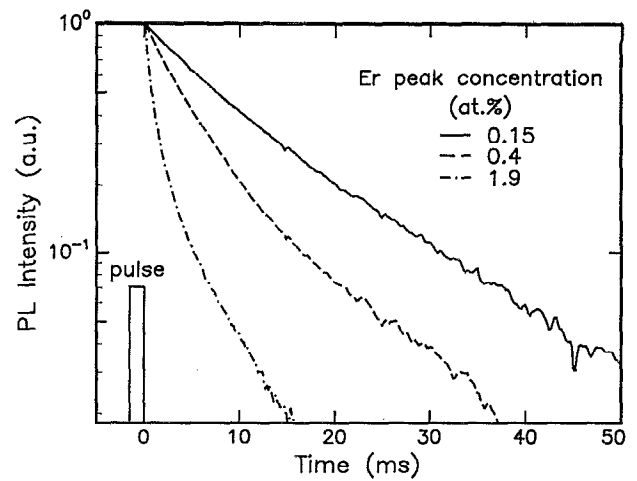


FIG. 6. PL decay curves after a 1.5 ms excitation pulse. The samples were implanted with 1.3 , 3.7 , and $18 \times 10^{15} \text{Er}/\text{cm}^2$ (0.15, 0.4, and 1.9 at. % peak concentration) and annealed at 512°C . The luminescence intensity at $\lambda = 1.537 \mu\text{m}$ is plotted on a logarithmic scale. The excitation pulse is indicated schematically.

signals with different decay times corresponding to different concentrations. However, attempts to fit the curves in Fig. 6 by integrating over the Gaussian profile using a function relating lifetime to concentration did not yield results consistent for all decay curves. Therefore, other processes leading to nonexponential decay at high concentration must also play a role.

Figure 7 shows the dependence of PL intensity on pump power, measured for three Er peak concentrations (0.15, 0.4, and 1.9 at. %) after annealing at 512°C . The dashed lines show the linear extrapolation of the first six datapoints. At higher pump intensity the measured curves

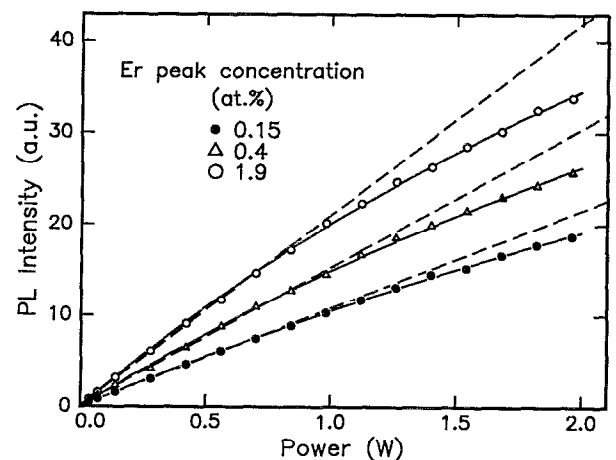


FIG. 7. PL intensity at $\lambda = 1.537 \mu\text{m}$ measured as function of pump power at 514.5nm . The samples were implanted with 1.3 , 3.7 , and $18 \times 10^{15} \text{Er}/\text{cm}^2$ and were annealed at 512°C . The dashed lines are linear extrapolations of the first six datapoints. The solid line drawn for 0.15 at. % is calculated using Eq. (2); the other two solid lines guide the eye. A power of 2.0 W corresponds to an intensity of $\sim 3 \text{kW}/\text{cm}^2$.

start to deviate from the linear extrapolation. At 2.0 W (corresponding to an intensity of $\sim 3 \text{ kW/cm}^2$) the signal from the sample with 0.15 at. % Er peak concentration is 12% lower than the linear extrapolation. This deviation increases with Er fluence, and for 1.9 at. % Er the PL signal is 20% lower than the linear extrapolation. The PL lifetimes (data not shown) do not depend on pump power up to 2.0 W.

IV. DISCUSSION

The experimental results show that soda-lime-silicate glass can be optically doped with Er by ion implantation. The spectral shape (Fig. 3) is a result of transitions between different Stark levels of the $^4I_{13/2}$ and $^4I_{15/2}$ manifolds,¹² in combination with homogeneous and inhomogeneous broadening. The $^4I_{13/2}$ manifold is populated through successive nonradiative relaxation from the $^2H_{11/2}$ pump level. The spectrum is broader than observed for Er-implanted pure silica,¹⁰ which is characteristic for a multicomponent host glass.⁹ An advantage of the relatively large spectral width is that optical amplification will be possible over a large bandwidth. The low-wavelength shoulder peaks at $1.48 \mu\text{m}$, a wavelength at which commercial pump lasers are available. This may allow for resonant pumping.

Ion implantation in glass creates structural damage, either by nuclear collisions, or by electronic excitations.¹¹ Structural defects can quench the parity-forbidden (intra- $4f$)—and therefore long lived—radiative transition, as they cause nonradiative decay channels.¹³ As a result the PL decay time and intensity decrease. In first approximation, for a concentration C_a of optically active (trivalent) Er, the measured lifetime (τ) and PL intensity (I) are given by

$$\frac{1}{\tau} = W_r + W_{nr} \quad \text{and} \quad I \propto \frac{\tau}{\tau_r} C_a, \quad (1)$$

where $W_r = 1/\tau_r$ and W_{nr} are the radiative- and nonradiative decay rates, respectively. Assuming that W_r is constant,¹⁴ Eq. (1) shows that a high nonradiative decay rate leads to a low lifetime (τ) and a proportionally low PL intensity. This proportionality is observed for the samples used in Fig. 4. For each sample the PL lifetime after annealing at 512°C is twice as long as after 400°C annealing (data not shown), which indeed corresponds to the observed doubling of PL intensity above 400°C . The fact that the changes in intensity fully correspond to the observed lifetime changes implies that the active fraction of Er (C_a) does not change on annealing. The lifetime increase on annealing is attributed to annihilation of ion-beam-induced defects in the silicate network.^{11,13,15} The required annealing temperature to optimize the Er luminescence ($\sim 500^\circ\text{C}$) is lower than that for Er-implanted pure silica.¹⁰ This may be related to the fact that soda-lime-silicate glass has a lower transformation temperature than pure silica.¹⁶

The saturation of the PL intensity for increasing Er fluence (Fig. 5) can be attributed to changes in the non-

radiative decay rate. The intensity from a sample with $1.8 \times 10^{16} \text{ Er/cm}^2$ is almost equal to the intensity at $6 \times 10^{15} \text{ Er/cm}^2$, although three times more Er was implanted. The lifetime, however, has decreased by a factor of three, thereby keeping the product τC_a in Eq. (1) constant. The dashed line in Fig. 5 was derived from the solid line through the lifetime data, by calculating the product τC_a . It shows perfect agreement with the PL intensity data over the full concentration range. The decrease in PL lifetime for high concentration is attributed to processes in which the excitation migrates through the glass by resonant exchange between closely spaced Er ions until a quenching center is met. These effects have been studied in detail in other materials doped with rare earths^{17,18} and usually become significant at concentrations above 0.1 at. %. This concentration quenching effect limits the concentration of Er that can be incorporated usefully in soda-lime-silicate glass. The optimum product of lifetime and intensity is reached at an Er peak concentration of ≈ 0.4 at. %.

For future use of these heavily doped silica glass films in planar optical waveguides, the behavior as a function of pump intensity is an important parameter (Fig. 7). As a first approach the sublinear increase of PL with pump intensity is a result of the depletion of Er ions in the ground state. The fraction of excited Er ions, N_2 , in a simple two-level system pumped at a rate R is

$$N_2 = \frac{R\tau}{1+R\tau}, \quad \text{with} \quad R = \frac{I_p}{h\nu} \sigma_a. \quad (2)$$

Here, $h\nu$ is the energy of the pump photons, I_p denotes the pump intensity, and σ_a the absorption cross section. Equation (2) shows that N_2 (and therefore the $1.54 \mu\text{m}$ PL intensity) is sublinear in I_p , and that the sublinearity is less for samples with shorter lifetime τ . However, Fig. 7 shows an opposite behavior: The samples with a high concentration, i.e., short lifetime deviate more from the straight line than the samples with a low concentration, i.e., long lifetime. This suggests that another nonradiative process, which is related to both pump intensity and Er concentration, must be present. One possible explanation is that cooperative upconversion takes place,¹⁷ in which energy is transferred nonradiatively from one excited Er ion to a neighboring excited Er ion, promoting the latter to the $^4I_{9/2}$ level (see Fig. 1). From $^4I_{9/2}$ the most probable decay is back to the $^4I_{13/2}$ manifold, via the $^4I_{11/2}$ level. As a result, the $\lambda = 1.54 \mu\text{m}$ PL is quenched at high pump intensities. From the data in Fig. 7 an upperlimit of the absorption cross section for Er^{3+} in soda-lime-silicate glass at 514.5 nm can be obtained by fitting Eq. (2) through the data for the lowest Er concentration. This yields $\sigma_a = 2 \times 10^{-21} \text{ cm}^2$, a typical value for Er in a multicomponent glass.⁹

V. CONCLUSIONS

Erbium-implanted (500 keV) soda-lime-silicate glass shows clear photoluminescence (PL) around $1.54 \mu\text{m}$ with a relatively large spectral width of 19 nm. Thermal annealing at a temperature above 500°C , causing annihilation of

implantation-induced defects, is necessary to optimize PL properties. The PL intensity first increases with Er fluence, but saturates above $\sim 6 \times 10^{15}/\text{cm}^2$. The saturation is explained by a decrease of PL lifetime with increasing concentration. The lifetime decrease is attributed to concentration quenching, as a result of energy exchange among closely spaced Er ions. The optimum Er concentration is found to be ≈ 0.4 at. %, for which the PL lifetime is 6 ms. The dependence of PL intensity on pump intensity shows evidence for an additional quenching mechanism related to high concentrations of excited Er^{3+} , possibly cooperative upconversion. With these parameters, Er-implanted soda-lime-silicate glass waveguides with a length of typically several cm may produce optical gain.

ACKNOWLEDGMENTS

We thank J. S. Custer for his contribution to the experimental setup and help in the analysis. We have greatly benefitted from discussion with M. B. J. Diemeer and B. Hendriksen from PTT Research, Leidschendam, The Netherlands. This work is part of the research program of the Foundation for Fundamental Research on Matter (FOM), and was made possible by financial support from the Dutch Organization for the Advancement of Pure Research (NWO), the Netherlands Technology Foundation (STW), and the IC Technology Program (IOP Electro-Optics) of the Ministry of Economic Affairs.

- ¹B. J. Ainslie, *J. Lightwave Technol.* **9**, 220 (1991).
- ²E. Desurvire, J. R. Simpson, and P. C. Becker, *Opt. Lett.* **12**, 888 (1987).
- ³C. H. Henry, G. E. Blonder, and R. F. Kazarinov, *J. Lightwave Technol.* **7**, 1530 (1989).
- ⁴J. Shmulovich, A. Wong, Y. H. Wong, P. C. Becker, A. J. Bruce, and R. Adar, *Electron. Lett.* **28**, 1181 (1992).
- ⁵T. Kitagawa, K. Hattori, M. Shimizu, Y. Ohmori, and M. Kobayashi, *Electron. Lett.* **27**, 334 (1991).
- ⁶G. Kitagawa, K. Hattori, K. Shuto, M. Yasu, M. Kobayashi, and M. Horiguchi, *Proceedings of the Topical Meeting on Optical Amplifiers and their Applications (OSA)*, Santa Fe, NM, 1992.
- ⁷R. V. Ramaswamy and R. Srivastava, *J. Lightwave Technol.* **6**, 984 (1988).
- ⁸M. M. Abouelleil, G. A. Ball, W. L. Nighan, and D. J. Opal, *Opt. Lett.* **16**, 1949 (1991).
- ⁹W. J. Miniscalco, *J. Lightwave Technol.* **9**, 234 (1991).
- ¹⁰A. Polman, D. C. Jacobson, D. J. Eaglesham, and J. M. Poate, *J. Appl. Phys.* **70**, 3778 (1991).
- ¹¹P. Mazzoldi and G. W. Arnold, in *Ion Beam Modification of Insulators*, edited by P. Mazzoldi and G. W. Arnold (Elsevier, Amsterdam, 1987), Chap. 5.
- ¹²S. Hufner, *Optical Spectra of Transparent Rare-Earth Compounds* (Academic, New York, 1978).
- ¹³A. Polman, D. C. Jacobson, and J. M. Poate, *Mater. Res. Soc. Symp. Proc.* **235**, 377 (1992).
- ¹⁴This is suggested by the observation that the spectral shape is independent of fluence and annealing temperature.
- ¹⁵A. Polman, D. C. Jacobson, A. Lidgard, and J. M. Poate, *Nucl. Instrum. Methods B* **59/60**, 1313 (1991).
- ¹⁶H. Scholze, *Glass* (Springer, Heidelberg, 1990).
- ¹⁷J. C. Wright, in *Radiationless Processes in Molecules and Condensed Phases*, edited by F. K. Fong (Springer, Heidelberg, 1976), Chap. 4.
- ¹⁸W. Ryba-Romanowski, *J. Lumin.* **46**, 163 (1990).